

# How Graphene-like is Epitaxial Graphene? Quantum Oscillations and Quantum Hall Effect

Johannes Jobst,<sup>1</sup> Daniel Waldmann,<sup>1</sup> Florian Speck,<sup>2</sup> Roland Hirner,<sup>2</sup>  
Duncan K. Maude,<sup>3</sup> Thomas Seyller,<sup>2</sup> and Heiko B. Weber<sup>1,\*</sup>

<sup>1</sup>*Lehrstuhl für Angewandte Physik, Universität Erlangen-Nürnberg, 91056 Erlangen, Germany*

<sup>2</sup>*Lehrstuhl für Technische Physik, Universität Erlangen-Nürnberg, 91056 Erlangen, Germany*

<sup>3</sup>*Laboratoire des Champs Magnétiques Intenses, 25 Avenue des Martyrs, 38042 Grenoble, France*

(Dated: November 23, 2018)

We investigate the transport properties of high-quality single-layer graphene, epitaxially grown on a 6H-SiC(0001) substrate. We have measured transport properties, in particular charge carrier density, mobility, conductivity and magnetoconductance of large samples as well as submicrometer-sized Hall bars which are entirely lying on atomically flat substrate terraces. The results display high mobilities, independent of sample size and a Shubnikov-de Haas effect with a Landau level spectrum of single-layer graphene. When gated close to the Dirac point, the mobility increases substantially, and the graphene-like quantum Hall effect occurs. This proves that epitaxial graphene is ruled by the same pseudo-relativistic physics observed previously in exfoliated graphene.

Graphene, a single sheet of graphite, is one of the most exciting electronic materials in the last years [1]. The observation of very fast charge carriers even at room temperatures and unconventional quantum mechanics has stimulated far reaching visions in science and technology. Many of these properties are a direct consequence of the unique symmetry of graphene and its true two-dimensionality. A calculation of the single-particle band structure delivers a linear  $E(k)$  dispersion relation and a chiral degree of freedom in the electronic wave function. This *graphene physics* modifies, for example, the quantum Hall effect (QHE) [2, 3] and efficiently suppresses backscattering of charge carriers [4, 5, 6].

There are today two main preparation strategies for graphene, resulting in different materials. *Mechanical exfoliation* of single graphene sheets from graphite yields small flakes a few tens of microns in size which are usually deposited on a silicon wafer covered by a layer of silicon oxide allowing for electrostatic gating. Since its discovery in 2004, *exfoliated graphene* has been the driving force for the exploration of graphene physics. Remarkably, a broad agreement between experiment and theory has been observed.

The second strategy is *epitaxial growth* of graphene on well defined surfaces. This procedure promises large-scale fabrication, detailed surface-science control, and would offer technological perspectives. Epitaxial graphene is currently developed into two major directions. Chemical vapor deposition on Ni, for instance, has been demonstrated to lead to graphene flakes which could be transferred to an insulating substrate. In this case, QHE typical for graphene was observed [7]. Another method uses the temperature-induced decomposition of the wide-band gap semiconductor silicon carbide (SiC) [8, 9, 10]. Since SiC can be obtained in an insulating state, this technique

does not require transferring the graphene layer onto another substrate, which is a clear technological advantage.

Epitaxial growth on SiC has been carried out on both polar surface orientations. Not unexpected, the growth and the resulting layers are dissimilar in many aspects. On the carbon terminated surface (C-face) the decomposition is rapid and often multilayers are grown. Transport studies of multilayered epitaxial graphene (MLEG) on the C-face of SiC have shown SdH-oscillations of graphene monolayers and high electron mobility, but no QHE [9], which is a consequence of the mutual rotation of the graphene layers within the stack [11, 12]. On the silicon-terminated face (Si-face), growth of graphene is slower allowing for a controlled single-layer growth. The better thickness control achieved on Si-face SiC substrates yielding single layers is of particular importance for top-gated field effect devices as compared to thick stacks of MLEG [13] due to screening.

As a consequence, we have concentrated on the growth of single layer graphene on Si-face SiC. We studied extensively its surface with angle resolved photoemission (ARPES), scanning tunneling microscopy, low energy electron diffraction, Raman spectroscopy, and first transport experiments [10]. Altogether a picture has been developed that this material has excellent quality and fits well to the graphene-model band structure. An anomaly in the ARPES spectra of epitaxial graphene on SiC(0001) has been interpreted as the signature of many-particle interactions [14]. However, a different interpretation of ARPES [15] results suggest a symmetry breaking between A and B sublattices of graphene and subsequent formation of a band gap induced by the presence of the so-called buffer layer or  $(6\sqrt{3} \times 6\sqrt{3})R30^\circ$  reconstruction. The latter forms the intrinsic interface between SiC(0001) and thermally grown graphene. The interface layer is semi-conducting, i.e. has no states at the Fermi level, and we have proposed that it consists of a covalently bound graphene layer [16]. The higher order commensurate unit cell (supercell) of the combined system

---

\*Electronic address: Heiko.Weber@physik.uni-erlangen.de

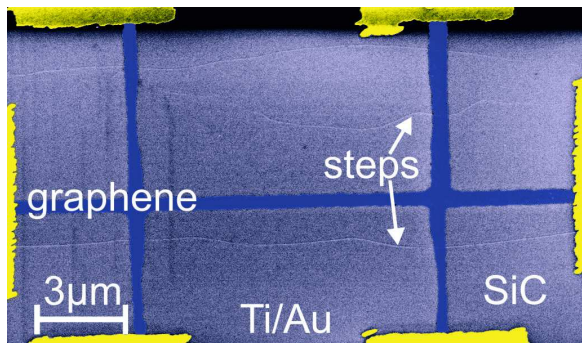


FIG. 1: Scanning electron micrograph of a Hall bar (0.48  $\mu\text{m}$  width) lithographically patterned out of a single layer of graphene (dark blue) on an atomically flat substrate terrace of semi-insulating SiC. The substrate steps are clearly resolved.

graphene on buffer layer on SiC(0001) contains  $13 \times 13$  unit cells of graphene. It remains an unresolved question, whether this lowered symmetry spoils the graphene physics by, e.g. inducing a band gap.

To discover the graphene physics in our system, we carried out classical Hall effect, Shubnikov-de Haas (SdH) effect and QHE measurements. The latter phenomena give a fingerprint of single-layer graphene behavior [17], clearly different from parabolic band structures or non-chiral wave functions. We investigated the raw material as well as epitaxial graphene driven close to charge neutrality by chemical gating.

The growth process and the patterning has been reported in [10]. Briefly, we have produced graphene on the silicon-terminated side of semi-insulating SiC by thermal decomposition at  $1650^\circ\text{C}$  and 900 mbar argon atmosphere for  $\approx 15$  min. Then we have removed the graphene partly by electron beam lithography and subsequent oxygen plasma etching, such that Hall bars of different sizes were patterned. Fig. 1 shows a Scanning electron micrograph of a sample with the Hall bar entirely placed on a single, atomically flat substrate terrace of the SiC(0001) surface. Here, we obtain reliably single-sheet graphene, as we keep some distance from the step edges [10]. Other samples were much larger, included many substrate steps and some even visible defects.

The electrical contacts were guided away from the Hall bar by graphene leads, and further out with metallic top contacts (Ti/Au). The samples were investigated in a cryostat fitted with a 0.66 T magnet, or in the high-field laboratory in Grenoble in magnetic fields up to 28 T.

The quantities which can be derived from Hall bar measurements are charge carrier densities and charge carrier mobilities. Figure 2 shows data derived for 51 samples of different sizes with the raw material. The charge carrier density of  $n \approx 10^{13} \text{ cm}^{-2}$  and a mobility at room temperature of  $\mu \approx 900 \text{ cm}^2/\text{Vs}$  is found for all samples. The charge carrier density can be related to electron-like transport with a chemical potential  $\approx 380 \text{ meV}$  above the Dirac point. This value is slightly below the photoemis-

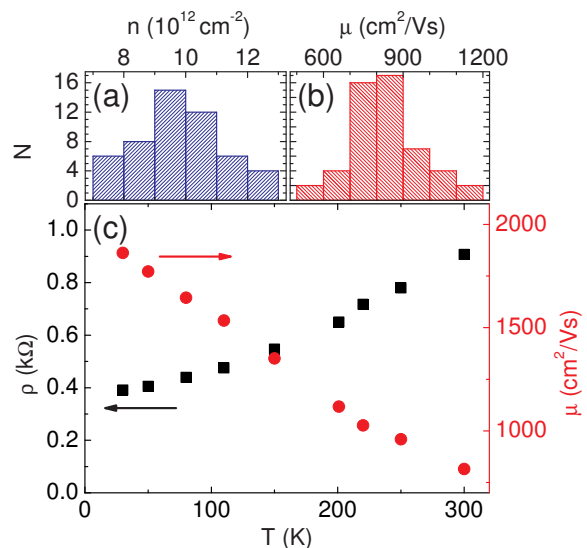


FIG. 2: a),b) Histograms of charge carrier density  $n$  and charge carrier mobility  $\mu$  in epitaxial graphene for 51 samples of various sizes at room temperature. Both quantities have been determined by Hall effect measurements. c) Temperature dependence of resistivity  $\rho$  and mobility  $\mu$  of a typical Hall-bar sample. The resistivity increases super-linearly with increasing  $T$ , while  $\mu$  decreases linearly

sion result of  $\approx 450 \text{ meV}$  [10]. Surprisingly, the mobility of rather large samples and of Hall bars placed on a single substrate step does not differ noticeably. Although it is known that graphene grows over step edges without being disrupted [9, 18], it is surprising that the inhomogeneity does not affect global transport properties significantly.

Graphene is a very surface sensitive material. Hence, one may believe that the limitation of mobility might be caused by surface adsorbates. We heated up four samples to  $350^\circ\text{C}$  for 30 min in cryogenic vacuum, in order to desorb potential adsorbates and continued the measurement without breaking the cryogenic vacuum. The measured quantities  $n$  and  $\mu$  remained essentially unaltered. Hence, adsorbates do not play a major role in our experiments. Further insight is gained from the temperature dependence of resistivity. It shows a super-linear behavior as reported for exfoliated graphene [19], but the temperature-dependent contribution  $\Delta\rho = \rho(300 \text{ K}) - \rho(0 \text{ K}) \approx 500 \Omega$  is one order of magnitude larger. Hence, even if the residual resistivity  $\rho(0 \text{ K})$  could be eliminated by improved sample preparation, the temperature dependent scattering mechanism would limit the room temperature mobility to  $\mu(300 \text{ K}) \approx 1600 \text{ cm}^2/\text{Vs}$ .  $\rho(0 \text{ K})$  presumably stems from imperfections, and may be related to atomically sharp defects (a nonvanishing amplitude of the D peak has also been observed in Raman spectroscopy [10]) while we attribute  $\Delta\rho$  to interactions with substrate phonons. Note also that the mobility plotted against  $T$  is remarkably linear.

In a further experiment, we measured the magnetoresistance in higher magnetic fields up to 28 T at cryogenic

temperatures ( $1.4\text{ K} < T < 4.2\text{ K}$ ). In this regime, electronic degrees of freedom are condensed in Landau levels, which have in graphene a significantly different spectrum compared to other materials [17]. Figure 3(a) shows the magnetoresistance  $R_{xx}$  and the Hall resistance  $R_{xy}$  as a function of magnetic field  $B$ . With increasing field, the evolution of  $R_{xx}$  to quantum oscillations can clearly be seen. The quantum Hall regime, however, with  $R_{xx} = 0$  is not yet reached in this sample with a charge density  $n = 8.9 \cdot 10^{12}\text{ cm}^{-2}$  and  $\mu = 2300\text{ cm}^2/\text{Vs}$ .  $R_{xy}$  already displays plateaus, which are precursors of the quantum Hall effect.

The values of these plateaus fit in the scheme of  $R_{xy} = h/(4n + 2)e^2$  with  $n$  being the Landau level index, as found in exfoliated graphene. When the positions of the associated maxima (minima) in  $R_{xx}$  are plotted against the inverse field  $1/B$  (Fig. 5), a linear dependence can be recognized. The axis intercept is  $\beta = n(B \rightarrow \infty) = 1/2$  ( $\beta = 0$ ), as expected and experimentally confirmed for electrons in exfoliated graphene (often, this is described as the geometric Berry phase  $\pi$  associated to a closed orbit). Hence, the SdH oscillations in the raw material (380 meV above the charge neutrality point) display graphene physics. Note that the expectations of the Berry phase in bilayer graphene would be  $2\pi$ .

The most interesting part of the graphene spectrum is the Dirac point, or the charge neutrality point, where the density of state shrinks to zero, and the charge carrier mobility may become huge [3]. In order to reach this point, we deposited tetrafluoro-tetracyanoquinodimethane (F4-TCNQ) molecules by thermal evaporation. Upon contact the strongly electronegative molecules expel electrons from the graphene and effectively drive the graphene close to the charge neutrality point [21]. We have chosen a thickness of several monolayers, for which the sample is reasonable stable. However, some drift in  $n$  occurs within days, accompanied by increasing inhomogeneities [20]. Classical Hall effect measurements of the sample with the lowest  $n = 5.4 \cdot 10^{10}\text{ cm}^{-2}$  displayed excellent mobilities of  $\mu = 29000\text{ cm}^2/\text{Vs}$  at  $T = 25\text{ K}$ , as shown in Fig. 4. Note that for rising temperatures, not only electrons, but also hole states are accessible by the Fermi distribution. As a consequence, the evaluation of the Hall data has to consider two charge carrier types, so  $\mu$  and  $n$  can not be unambiguously derived. When assuming a two-band model ( $\mu_{holes} = \mu_{electrons}$  for simplicity), the resulting simulation describes the temperature dependence reasonably well. The expectation would be that even higher mobilities are achievable, if one would come closer to the Dirac point. Mobilities over  $20000\text{ cm}^2/\text{Vs}$  are rarely found for exfoliated graphene on a substrate, and significantly better values are only found in absence of a substrate [22]. Here, high mobilities are observed although the graphene is in contact with two surfaces: the SiC substrate with its large supercell and the virtually disordered F4-TCNQ film on top.

For the measurements in high magnetic fields, we

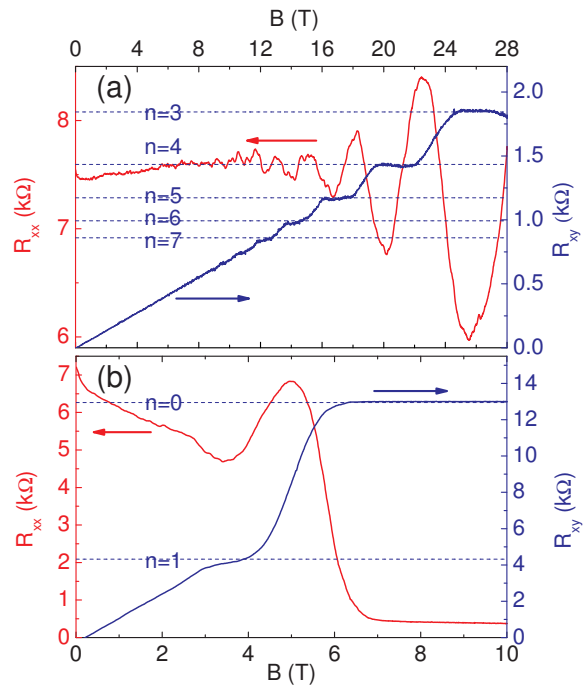


FIG. 3: (a) Resistance  $R_{xx}$  and Hall Resistance  $R_{xy}$  at  $T = 4.2\text{ K}$  from a sample of single-sheet graphene, entirely placed on a single substrate step (Fig. 1).  $R_{xx}$  shows Shubnikov-de Haas oscillations, but no quantum Hall effect. The Hall resistance, however, shows step-like plateaus like in the quantum Hall effect. Plateau values and the positions of extrema can be identified with the unconventional Landau-level structure of single-layer graphene. (b) The same quantities in a sample close to charge neutrality. Shubnikov-de Haas oscillations (barely visible below 4 T) and quantum Hall effect are present and demonstrate the unique single-layer graphene properties. Note that due to a lost contact during the experiment, the measurement was carried out as a three-terminal measurement. Hence, the quantum Hall resistance is  $R_{xx} \approx 300\ \Omega$  including the wire resistance, whereas  $0\ \Omega$  would be expected in a four wire experiment. In a further control experiment, we could verify with a slightly degraded sample that the sample indeed showed  $R_{xx} \approx 0\ \Omega$  at the quantum Hall plateau [20].

used another F4-TCNQ covered graphene sample. It was slightly filled with electrons ( $n = 4.9 \cdot 10^{11}\text{ cm}^{-2}$ ,  $\mu = 4900\text{ cm}^2/\text{Vs}$  at  $T = 4.2\text{ K}$ ). Figure 3(b) shows the magnetoresistance  $R_{xx}$  and the Hall resistance  $R_{xy}$ . In the low field regime, Shubnikov-de Haas oscillations occur. Compared to Fig. 3(a), the quantum oscillations are rather compressed as a consequence of the low charge carrier density. For magnetic fields larger than 7 T, the resistance is effectively zero, whereas the Hall resistance has the value  $h/2e^2$ . This is the last plateau of the QHE. From this single plateau, it can be derived that the QHE is different from bilayer graphene, where it should be  $h/4e^2$ . Further information about the Landau level spectrum can be gained by analyzing the SdH oscillations similar to the above procedure: a SdH phase is found which corresponds to a Berry phase of  $\pi$  (Fig. 5). It is

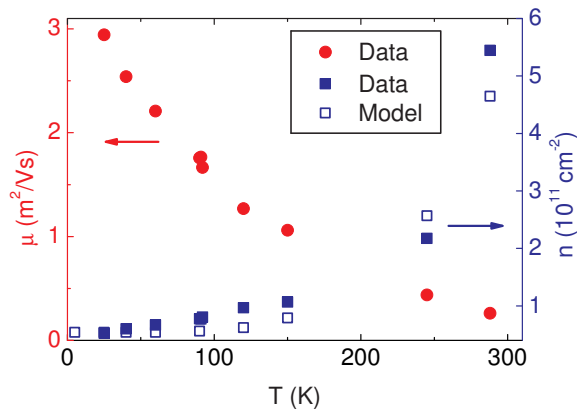


FIG. 4: Charge carrier mobility  $\mu$  and -density  $n$  for a sample close to the charge neutrality point ( $E_F = 27$  meV). Closed symbols:  $\mu$  (red) and  $n$  (blue) derived from an evaluation of Hall data, assuming only one charge-carrier type, yields mobilities of  $29\,000\text{ cm}^2/\text{Vs}$ . The strong temperature dependence comes from the interplay of electrons and holes in the Fermi distribution at finite temperatures. A simple two-band model (open squares) yields a similar  $T$  dependence.

remarkable that all samples show quantum oscillations typical for single-layer graphene, although the F4-TCNQ covered Hall bar as well as one as-prepared sample did not lie on a single substrate terrace and therefore parts of the sample are bilayers, which extend as small stripes along the step edges.

We conclude that the raw graphene material, which is strongly electron filled has a charge carrier mobility around  $900\text{ cm}^2/\text{Vs}$  at room temperature and  $2000\text{ cm}^2/\text{Vs}$  at low temperatures. This limitation comes partly from electron-phonon interaction with substrate phonons, partly from crystal imperfections. The mobility is insensitive to substrate steps. Shubnikov-de Haas oscillations and plateaus in the Hall resistance indicate that at  $B = 28$  T the quantum Hall regime is not yet fully reached, but the Landau-level spectrum is (single-sheet) graphene-like.

When gating close to the Dirac point, high mobilities of  $29\,000\text{ cm}^2/\text{Vs}$  are observed. The quantum oscillations in high magnetic fields reveal the Landau-level spectrum of single-sheet graphene, and the quantum Hall effect is observed. Hence, epitaxial graphene reproduces the unique features observed in exfoliated graphene, but is certainly a system which allows for more systematic development of graphene devices, with rich perspectives for science and technology.

We gratefully acknowledge support by the DFG under contract SE 1087/5-1, WE 4542-5-1, and within the Cluster of Excellence *Engineering of Advanced Materials* (www.eam.uni-erlangen.de). This work has been partially supported through EUROMAGNET II under SP7 of the EU; contract number 228043

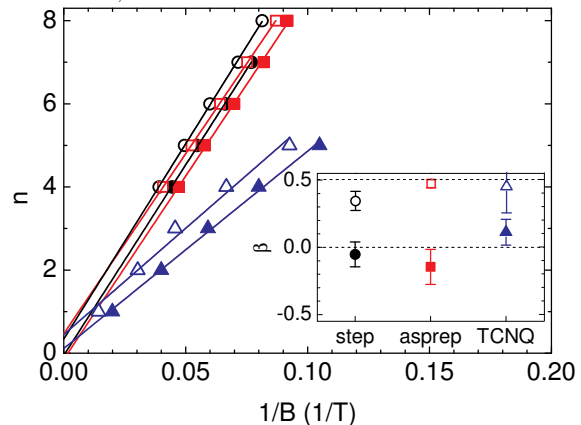


FIG. 5: Landau level index  $n$  of the SdH maxima (closed symbols) and minima (open symbols) over the inverse magnetic field  $1/B$  and linear fits. Circles: as-prepared sample lying on a single substrate terrace. Squares: as-prepared sample covering several substrate steps. Triangles: sample gated close to charge neutrality with F4-TCNQ (plotted against  $0.1/B$  for clarity). Inset: The axis intercepts of  $\beta = 0.5$  and  $\beta = 0$  for minima and maxima respectively yield a Berry phase of  $\pi$  as expected for single-layer graphene. The error bars indicate the standard deviation of the fitting constant.

- 
- [1] A. K. Geim and K. S. Novoselov, *Nature Materials* **6**, 183 (2007).
- [2] K. S. Novoselov, A. K. Geim, S. V. Morozov, D. Jiang, M. I. Katsnelson, I. V. Grigorieva, S. V. Dubonos, and A. A. Firsov, *Nature* **438**, 197 (2005).
- [3] Y. Zhang, Y.-W. Tan, H. L. Stormer, and P. Kim, *Nature* **438**, 201 (2005).
- [4] T. Ando and T. Nakanishi, *J. Phys. Soc. Jpn.* **67**, 1704 (1998).
- [5] M. I. Katsnelson, K. S. Novoselov, , and A. K. Geim, *Nature Phys.* **2**, 620 (2006).
- [6] A. F. Young and P. Kim, *Nature Phys.* **5**, 101 (2009).
- [7] K. S. Kim, Y. Zhao, H. Jang, S. Y. Lee, J. M. Kim, K. S. Kim, J.-H. Ahn, P. Kim, J.-Y. Choi, and B. H. Hong, *Nature* **457**, 706 (2009).
- [8] I. Forbeaux, J.-M. Themlin, and J.-M. Debever, *Phys. Rev. B* **58**, 16396 (1998).
- [9] C. Berger, Z. Song, X. Li, X. Wu, N. Brown, C. Naud, D. Mayou, T. Li, J. Hass, A. N. Marchenkov, et al., *Science* **312**, 1191 (2006).
- [10] K. V. Emtsev, A. Bostwick, K. Horn, J. Jobst, G. L. Kellogg, L. Ley, J. L. McChesney, T. Ohta, S. A. Reshanov, J. Röhrl, et al., *Nature Materials* **8**, 203 (2009).
- [11] J. Hass, F. Varchon, J. E. Millan-Otoya, M. Sprinkle, N. Sharma, W. A. de Heer, C. Berger, P. N. First, L. Magaud, and E. H. Conrad, *Physical Review Letters* **100**, 125504 (2008).
- [12] S. Shallock, S. Sharma, and O. A. Pankratov, *Physical Review Letters* **101**, 056803 (2008).
- [13] J. Kedzierski, P.-L. Hsu, P. Healey, P. W. Wyatt, C. L.



- Keast, M. Sprinkle, C. Berger, and W. A. de Heer, *IEEE transactions on electronic devices* **55**, 2078 (2008).
- [14] A. Bostwick, T. Ohta, T. Seyller, K. Horn, and E. Rotenberg, *nature Physics* **3**, 36 (2007).
- [15] S. Y. Zhou, G.-H. Gweon, A. V. Fedorov, P. N. First, W. A. de Heer, D.-H. Lee, F. Guinea, A. H. C. Neto, and A. Lanzara, *Nature Materials* **6**, 770 (2007).
- [16] K. V. Emtsev, F. Speck, T. Seyller, L. Ley, and J. D. Riley, *Phys. Rev. B* **77**, 155303 (2008).
- [17] K. S. Novoselov, E. McCann, S. V. Morozov, V. I. Falko, M. I. Katsnelson, U. Zeitler, D. Jiang, F. Schedin, and A. K. Geim, *Nature Physics* **2**, 177 (2006).
- [18] P. Lauffer, K. V. Emtsev, R. Graupner, T. Seyller, L. Ley, S. A. Reshanov, and H. B. Weber, *Phys. Rev. B* **77**, 155426 (2008).
- [19] S. V. Morozov, K. S. Novoselov, M. I. Katsnelson, F. Schedin, D. C. Elias, J. A. Jaszczak, and A. K. Geim, *Phys. Rev. Lett.* **100**, 016602 (2008).
- [20] We will provide supporting material.
- [21] W. Chen, S. Chen, D. C. Qi, X. Y. Gao, and A. T. S. Wee, *J. Am. Chem. Soc.* **129**, 10418 (2007).
- [22] K. I. Bolotin, K. J. Sikes, J. Hone, H. L. Stormer, and P. Kim, *Phys. Rev. Lett.* **101**, 096802 (2008).